Developments and challenges in the manufacturing, characterization and scale-up of energetic nanomaterials – A review

van der Heijden, A. E.D.M.

DOI
10.1016/j.cej.2018.06.051

Publication date
2018

Document Version
Accepted author manuscript

Published in
Chemical Engineering Journal

Citation (APA)
van der Heijden, A. E. D. M. (2018). Developments and challenges in the manufacturing, characterization and scale-up of energetic nanomaterials – A review. *Chemical Engineering Journal*, *350*, 939-948. https://doi.org/10.1016/j.cej.2018.06.051

Developments and challenges in the manufacturing, characterization and scale-up of energetic nanomaterials – a review

A.E.D.M. van der Heijden [a,b]

[a] *Netherlands Organisation of Applied Scientific Research, Dept. Energetic Materials, P.O. Box 45, 2280 AA Rijswijk, The Netherlands, antoine.vanderheijden@tno.nl*

[b] *Delft University of Technology, Dept. Process & Energy, Section Intensified Reaction and Separation Systems, Leeghwaterstraat 39, 2628 CB Delft, The Netherlands*

List of abbreviations

AFM	Atomic force microscopy
ALD	Atomic layer deposition
AN	Ammonium nitrate
AP	Ammonium perchlorate
BET	Brunauer-Emmett-Teller
CL-20	2,4,6,8,10,12-Hexanitro-2,4,6,8,10,12-hexaazaisowurtzitane
CNT	Carbon nanotube
CSLM	Confocal scanning laser microscopy
DAAT	3,3'-azobis(6-amino-1,2,4,5-tetrazine)
DC	Direct current
DHT	3,6-di(hydrazino)-1,2,4,5-tetrazine
DiAT	3,6-diazido-1,2,4,5-tetrazine
DSC	Differential scanning calorimetry
DTA	Differential thermal analysis
EDX	Energy-dispersive X-ray spectroscopy

ESD	Electrostatic discharge
FOX-7	1,1-Diamino-2,2-dinitroethylene
GAP	Glycidyl azide polymer
HMX	1,3,5,7-Tetranitro-1,3,5,7-tetrazocane
HOPG	Highly-oriented pyrolytic graphite
LLM-105	2,6-Diamino-3,5-dinitropyrazine-1-oxide
MDNT	1-Methyl-3,5-dinitro-1,2,4-triazole
NC	Nitrocellulose
NP	Nitrophloroglucinol
NTO	3-Nitro-1,2,4-triazol-5-one
PBX	Polymer-bonded explosive
PEI	Polyethyleneimine
PMMA	Polymethylmethacrylate
PVAc	Polyvinyl acetate
RAM	Resonant acoustic mixing
RDX	1,3,5-Trinitro-1,3,5-trinitrotriazinane
RF	Resorcinol-formaldehyde
SDBD	Surface dielectric barrier discharge
SEM	Scanning electron microscopy
SHIM	Scanning helium ion microscopy
TATB	Triaminotrinitrobenzene
TEM	Transmission electron microscopy
TG	Thermogravimetry

TNT	2,4,6-Trinitrotoluene
UN	United nations
VMCC	Carboxy-functional terpolymer consisting of vinyl chloride (83%), vinyl acetate (16%), and maleic acid (1%)
XPS	X-ray photon spectroscopy
XRD	X-ray diffraction

Keywords

Energetic nanomaterials, manufacturing, characterization, scale-up.

Declarations of interest

None.

Abstract

In the domain of energetic nanomaterials, more specifically nano-sized explosives and oxidizers, many small scale production methods have been explored up to now. So far only limited attempts have been made to scale up the production to tens or maximally a few hunderds of grams. This paper provides a review of these small scale production methods as well as characterization techniques for nanometric explosives and oxidizers. As a result of the limited scale-up, the application of energetic nanomaterials in typical propellant and explosive formulations is currently very limited. This might be caused by the fact that a clear and commonly shared view on which energetic nanomaterials and production processes it would be economically beneficial and feasible to invest in is

lacking at the moment. Furthermore, a considerable number of technical challenges can be expected regarding the processing of energetic nanomaterials on a composition level. To manage these challenges, this review proposes several technical solutions which may contribute to a better understanding of the benefits, risks and costs involved in the use and scale-up of energetic nanomaterials and, if considered economically feasible, a more widespread application of these nanomaterials in the defense and space domains.

1. Introduction

Energetic materials store chemical energy within their molecular structure, which can be released in a very short time upon initiation by mechanical, thermal or chemical stimuli. An ideal energetic material combines high performance and high thermal stability on the one hand and a low sensitivity on the other. Energetic materials are widely applied in explosives, pyrotechnics and gun/rocket propellants. Apart from the energetic material itself, also other ingredients are required to manufacture an energetic formulation for practical applications. These ingredients are e.g. a polymeric binder (which can be a wax or paraffin), curing agents, plasticizers, curing catalysts, stabilizers, burning rate modifiers and a fuel. To be able to tune the performance, mechanical, thermal and ballistic properties of energetic formulations, the solid load and the choice of the polymeric binder system (comprising polymer, curing system and plasticizer) play an important role. By using bi- or trimodal size distributions of the energetic material and varying their ratio, the solid load can be optimized.

After the increase in the interest in nanomaterials and their gradual introduction in e.g. pharmaceutical [1], cosmetic [2] and catalytic products [3], nanomaterials also gained

more and more interest as an ingredient in energetic formulations [4]. The potential benefit of the use of nanomaterials was mainly related to the difference in physicochemical properties compared to conventionally sized particles as a result of the very high specific surface area. Specifically for energetic formulations, the (partial) replacement of conventionally sized particles with nanoparticles would be interesting for burning rate modifiers, catalysts, (metal) fuels and of course the energetic material itself. The use of nanoparticles allows to combine fuel and oxidizer particles at the nanometric scale where the rate of energy release is primarily controlled by chemical kinetics rather than by mass transport. For energetic materials applied as an explosive, it has been demonstrated that the shock initiation sensitivity is directly related to the quality of the explosive particles: the higher the averaged density of the particles, the lower the number of defects like inclusions and voids and the higher the shock initiation pressure [5]. The size of an inclusion is typically a few micron and larger. The prospect that the number of defects in nanoparticles can be reduced considerably compared to conventionally sized energetic materials, has been an important driver for the research and development on energetic nanomaterials since this is expected to lead to less sensitive energetic materials [6-12].

Many papers and reviews have dealt with the production, development, characterization and application of nano-sized metals and metal oxides for use in pyrotechnics (e.g. thermites) or nanometals like nano-Al as a fuel in explosives and solid composite rocket propellants [4, 13-15]. The review by Pessina and Spitzer [16] mainly focused on the crystallization of nano-RDX. In this review the scope will be broader, including

developments and challenges in the manufacturing, characterization and application of nanoparticles of both oxidizers and explosives.

Chapter 2 reviews the methods that have been developed for producing energetic nanomaterials. The characterization of energetic nanomaterials will be treated in Chapter 3. Finally, in chapter 4 the challenges and future outlook of this fascinating field will be discussed.

2. Production methods

An overview will be given of the currently available methods to manufacture energetic nanomaterials. The production methods will be divided into methods for manufacture of either single-component nanoparticles, or nano-sized cocrystals or for manufacture of nanocomposites.

2.1 Single-component energetic nanoparticles

Various production techniques have been developed to prepare single-component nanoparticles. An overview is given in Table 1. A few of these techniques share a common principle, i.e. solid particles are generated by first forming small solution droplets containing the material to be crystallized and subsequent evaporation of the solvent leading to nucleation and growth of the dissolved material. Spray drying [7], electrospray [10] and spray flash evaporation [11] depend on this principle. A (under)saturated solution is sprayed over a nozzle generating many small, practically monodisperse droplets. The size of these droplets is mainly determined by the diameter of the nozzle, the flow rate of the solution over the nozzle and the viscosity and surface

tension of the solution. Upon evaporation of the solvent, supersaturation is built up inside the droplets followed by nucleation of crystalline material. The remaining solvent continues to evaporate, leading to growth of the nucleated particles. The maximum size the particles are able to reach, is limited by the volume of the droplet and concentration of the energetic material. Since the droplets are practically monodisperse, also the nanoparticles usually show a narrow size distribution. Finally, once all solvent has evaporated, the nanoparticles can be collected on a surface. Barreto-Cabán et al. [7] used a spray drying technique to prepare RDX and TNT nanoparticles, starting from a solution in methanol, on a silicon substrate. In this way RDX with a mean size of 250-500 nm and a narrow size distribution could be produced. For TNT an even smaller mean size of 125-200 nm was found. In a different configuration Spitzer et al. [9] and Risse et al. [11] used an ultrasonic, piezoelectric transducer to produce an aerosol of an RDX/acetone solution. A flow of inert gas (e.g. nitrogen) carries the aerosol to a heating zone in which the acetone evaporates and the RDX crystallizes. The gas flow further carries the particles to an electrical precipitator, consisting of two electrodes to which a potential difference of 8-15 kV is applied. This charges the particles, which then deposit on the electrodes (mostly on the cathode, ca. 90 wt%). The resulting particles consist of micron-sized agglomerates built up from 15-100 nm sized individual particles.

Table 1: Overview of production methods developed for producing energetic nanomaterials (single components, cocrystals) and nanocomposites.

Production method	Type of product	Energetic material(s)	Reference(s) (examples)
Spray drying	Single components, nanocomposites	RDX, TNT, LLM-105, RDX	[7, 17, 18]

Spraying in a non-solvent or cryogenic solvent (liquid N_2)	Single components	NTO, HMX, CL-20	[6, 19-22]
Spray flash evaporation	Single components, cocrystals	RDX, 2CL-20:HMX, CL-20:TNT	[9, 11, 23]
Grinding / bead milling	Cocrystals, nanocomposites	2CL-20:HMX, TATB, HMX	[24, 25]
Electrospray	Single components	RDX, TNT, HMX, CL-20	[10, 26]
Rapid expansion of a supercritical solution (CO_2)	Single components	RDX, PETN, HNS	[27, 28]
Vacuum evaporation and condensation/deposition	Single components	RDX, AN, LLM-105	[29-31]
Micro-channel directional crystallization	Single components	TATB	[32]
Plasma-enhanced crystallization	Single components	RDX	[12]
Sol-gel / cryogel	Nanocomposites	CL-20/NC, AP/RDX, AP, HMX/AP, RDX/GAP, NC/RDX/AP	[33-38, 47-50]
Templates (HOPG, CNT, C_{60})	Nanocomposites	LLM-105	[31, 39, 40]

Sprayed droplets may merge after leaving the nozzle and this broadens the size distribution of the final product. To avoid droplet coagulation, a potential difference can be applied between the nozzle and the surface on which the particles are collected. During this so-called electrospray process (see Figure 1), the droplets are either positively or negatively charged, so they repel each other, which suppresses their coagulation. Also another effect plays an important role during electrospray: as the droplet reduces in size due to evaporation of the solvent, the surface charge density will gradually increase, leading to a critical charge density where new surface area must be created to reduce the charge density. This is called Coulomb fission and was first described by Rayleigh [41]. The Rayleigh limit describes the relation between the force that holds the droplet together

(determined by surface tension) and an opposing electrostatic force (determined by the surface charge density) that wants to break up the droplet as to create more surface area.

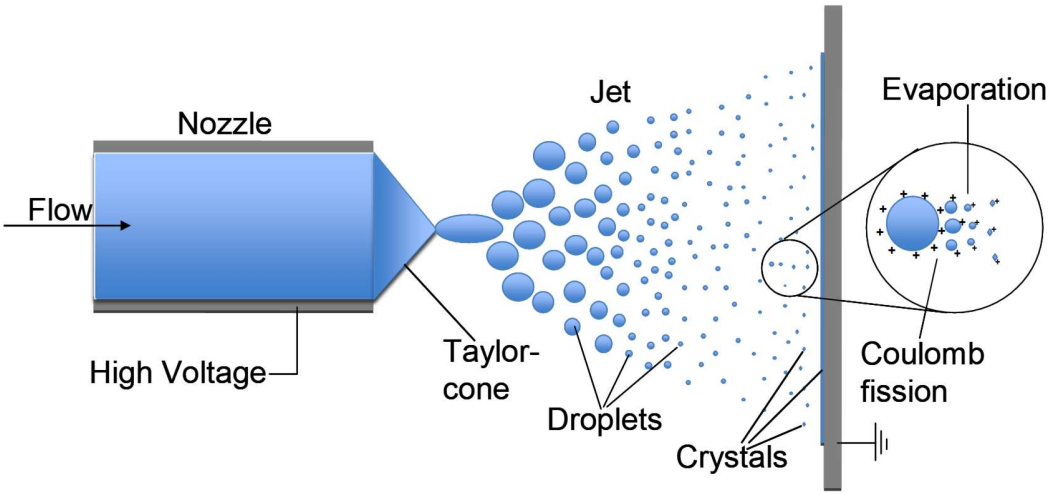

Figure 1: Process scheme of electrospray crystallization [10].

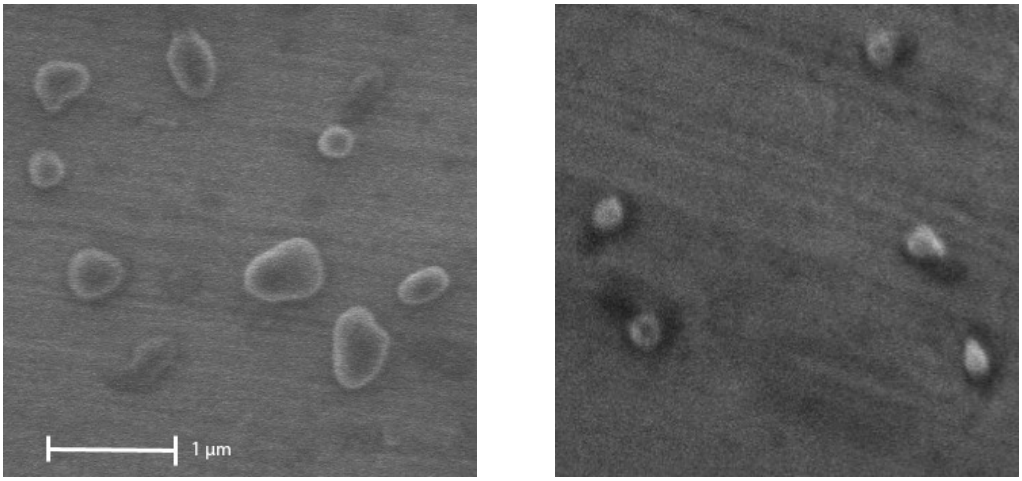

(a) (b)

Figure 2: Electrospray crystallization [10] of (a) RDX and (b) HMX. The size bar applies to both pictures.

The Coulomb fission effect therefore further reduces the size of the droplets, and in this way in principle also the average size of the nanoparticles. Results from an electrospray process [10] using an RDX/acetone solution, showed the formation of high-quality, submicron-sized RDX crystals with an average size of around 400 nm, see Figure 2(a). The influence of different process parameters like nozzle diameter, flow rate, potential difference, solution concentration and working distance (distance between nozzle and grounded collecting plate) on the mean particle size and size distribution were systematically investigated. Similarly, submicron HMX particles with an average size of 400 nm have been prepared by means of electrospray crystallization, see Figure 2(b).

Yongxu et al. [6] prepared reticularly structured HMX with an average grain size of 20-100 nm by spraying an HMX solution of varying concentrations in acetone into an organic non-solvent. Bayat et al. [20] used the same method and sprayed an HMX solution in acetone in a non-solvent (water) to control the mean size of the HMX crystals. They systematically varied the solution and non-solvent temperature, the addition of a surfactant (iso-propyl alcohol), the compressed air flow rate and the solution flow rate to study their effect on the mean size of the submicron HMX crystals. Similarly, by spraying a solution of CL-20 in ethyl acetate in a non-solvent (iso-octane) while efficiently stirring the non-solvent in the presence of ultrasound, Bayat and Zeynali [21] were able to produce nano-CL-20 particles with a mean size of 95 nm. Wang et al. [22] applied the same method to produce CL-20 particles, so including the use of ultrasound, but instead of iso-octane, n-hexane and n-heptane were used as non-solvent. This resulted in CL-20 particles within a size range of 300-700 nm. Instead of using an organic non-

solvent, a cryogenic non-solvent like liquid nitrogen or liquid carbon dioxide have been used. An example is the production of nano-NTO particles by spraying an aqueous NTO solution into liquid nitrogen [19]. After a freeze drying treatment to remove the (solidified) water, NTO particles in a size range of 50-100 nm were found.

The spray flash evaporation process [11] consists of a high- and low-pressure section that are connected via a hollow cone nozzle. In the high-pressure section a solution, containing the energetic material, is heated above its normal (atmospheric) boiling temperature. This solution is sprayed over the nozzle into the low-pressure section. There the solvent is flash-evaporated leading to crystallization of the dissolved energetic material. As a result of the combined temperature drop and evaporation effect, high supersaturation levels can be reached, which are essential for the formation of nanoparticles. In this way RDX particles with a mean size of 500 nm have been produced, starting with an RDX/acetone solution.

Supercritical CO_2 has also been used as a solvent. By rapidly expanding this supercritical solution over a nozzle, the supercritical solvent turns into a gas and the dissolved material crystallizes practically instantaneously. Stepanov et al. [28] developed a higher throughput process based on rapid expansion of a supercritical solution (RESS) to produce sufficient quantities for various initiation sensitivity tests. RDX powders with a mean size in the range of 200 to 500 nm were produced. Bishop et al. [27] reported on the use of RESS to produce PETN with a very high surface area, up to 8 m^2/g.

Apart from the above mentioned techniques based on spray drying, several other methods have appeared in literature. The first one is the production of nano-RDX and nano-AN via vacuum evaporation and condensation/deposition onto a cold quartz substrate. AN and RDX nanoparticles were formed with sizes around 50 nm [29, 30].

A similar concept was used by Yang et al. [31] where a small amount of LLM-105 (2,6-diamino-3,5-dinitropyrazine-1-oxide) powder was put on a sample plate. The temperature of the sample plate was raised to 220 °C at atmospheric pressure and kept constant for 20 min. A 1 cm^2 piece of highly oriented pyrolytic graphite (HOPG) substrate was cleaved and placed 15 cm above the LLM-105 sample for 40 s. The LLM-105 vapor was deposited on the surface of the HOPG substrate forming single-crystalline nanosheets of LLM-105 with a thickness of 50 nm and a lateral dimension of more than 1 μm.

Wang et al. [32] reported on a technique using micro-channel directional crystallization of TATB 3D structures. TATB was dissolved in sulfuric acid; by diffusion of water and sulfuric acid through a micro-channel interface, 3D-nanostructures of TATB were formed. By varying the growth time (1, 3, 4 and 6 hrs) and the channel diameters (3, 5, 10 and 200 nm), different sizes, structures and agglomerates could be made built up from smaller individual particles (mostly nanorods of a few tens up to 200 nm in length).

Finally, an atmospheric pressure cold surface dielectric barrier discharge (SDBD) plasma was used for the production of nano-sized RDX [12]. This method used a nebulizer to generate RDX/acetone solution droplets that were carried by high pressure argon gas to a

plasma reactor, see Figure 3. The plasma reactor consisted of two electrodes separated by a dielectric (Al_2O_3 ceramic plate, 1 mm thickness). One of the electrodes consisted of 20 interconnected 1 mm wide, 50 µm thick strips of platinum deposited on the ceramic plate. The gap between the electrode strips was 3 mm. By applying a DC bias voltage superposed on an alternating pulsed voltage between the counter and discharge electrodes, a plasma was formed in the gaps between the electrode strips. The cold plasma had two functions: it heated the droplets and therefore enhanced the evaporation rate of the acetone. Secondly, the plasma electrically charged the RDX/acetone droplets, again promoting Coulomb fission, as described above. In this way RDX particles in a size range of 200-900 nm could be produced, see Figure 4.

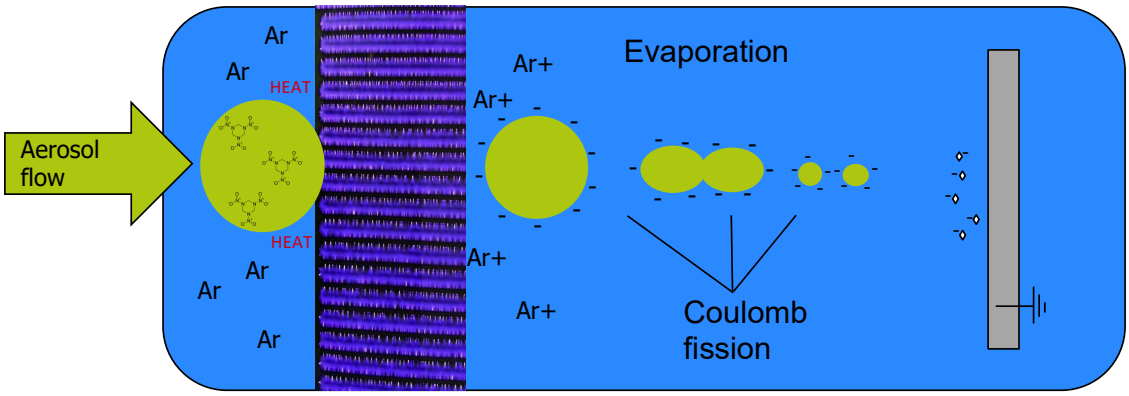

Figure 3: Process scheme of plasma aided crystallization [12].

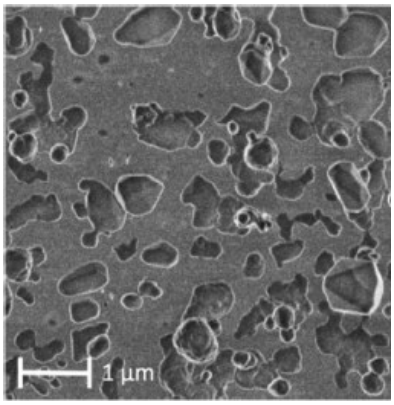

Figure 4: 200-900 nm RDX manufactured by means of plasma aided crystallization [12].

2.2 Nanometric energetic cocrystals

Cocrystals have been defined as solids that are crystalline, single phase materials composed of two or more different molecular and/or ionic compounds, generally in a stoichiometric ratio, which are neither solvates nor simple salts [42]. The development of cocrystals e.g. in the area of pharmaceutics appears to be a promising approach for energetic materials as well [43, 44], as they can offer a higher thermodynamic stability and tunable sensitivity and detonation properties. Because of the emerging interest in cocrystal development, this type of new materials is treated here as a separate class of materials.

Up to now, the scientific literature on nano-sized energetic cocrystals is still very limited. Ball or bead milling is a conventional technique with which cocrystals can be prepared. Due to the sensitive nature of energetic materials (specifically for friction and impact), ball milling is generally not a preferred technique. Nevertheless, Qiu et al. [24] succeeded in preparing a 2:1 (molar ratio) CL-20:HMX cocrystal by bead milling an aqueous

suspension of ε-CL-20 and β-HMX in a 2:1 stoichiometric ratio. After 60 min of milling, a mean size smaller than 200 nm was reached. The conversion from separate ε-CL-20 and β-HMX to the CL-20:HMX cocrystal seems to take place by a solvent-mediated phase transformation mechanism.

Using a resonant acoustic mixer (RAM) energetic cocrystals consisting of CL-20 and HMX in a 2:1 molar ratio [45] and CL-20 and 1-methyl-3,5-dinitro-1,2,4-triazole (MDNT) in a 1:1 molar ratio [46] have been prepared successfully. Unfortunately the mean size of these cocrystals was not reported in these papers. In a paper by Doblas et al. [23], results have been shown on nano-sized cocrystals of CL-20 with HMX and TNT using spray flash evaporation (described in section 2.1). They produced CL-20/TNT (equimolar) and CL-20/HMX (2:1) cocrystals with mean sizes of 100 and 58 nm, respectively.

2.3 Nanocomposite energetic materials

Nanocomposite (or nanostructured composite) energetic materials form another class of energetic nanomaterials. With a nanocomposite energetic materials we mean a composite consisting of nano-sized particles or nanolayers of fuel and oxidizer [4].

Several manufacturing techniques have been developed to make nanocomposite energetic materials. A relatively simple method is high-energy ball milling. In this way Zeng et al. [25] prepared nanocomposites of TATB and the fluorine resin F2311 and of TATB and HMX. Another, much more frequently applied method is the sol-gel technique. The sol-gel chemistry involves reactions of two or more chemicals in solution to produce nano-

sized primary particles ("sols"), which can be linked to form a three-dimensional solid network ("gel") containing pores filled with the remaining solution. After controlled evaporation of the remaining liquid phase, a dense, highly uniform porous solid is formed. This homogeneity ensures uniform material properties of the final nanocomposite structure [47]. The nano-sized primary particles may be formed after formation of the gel e.g. by inducing crystallization of the dissolved material by exchanging the liquid present in the pores for a solvent in which the material is insoluble. The sol-gel method can be combined with a cryogenic processing step where the sol-gel is quickly cooled down to liquid nitrogen temperatures after which the nanocomposite is formed due to freeze drying of the used solvent (also referred to as the cryogel method). This latter method has afforded higher solid loadings of the nanoparticles into the polymer matrix than might be the case with other sol-gel processing methods [33, 34]. Using the sol-gel method, the following nanocomposite energetic materials have been reported in literature: AP in a resorcinol-formaldehyde (RF) matrix [47], CL-20/NC [33, 34], AP/RF [35], AP/RDX/SiO_2 [36], AP/SiO_2 [48], RDX/AP in a matrix of phloroglucinol (P) and nitrophloroglucinol (NP) as precursors and formaldehyde as reagent [37], RDX/GAP [49] and NC/RDX/AP [50]. Instead of using liquid nitrogen in the cryogel method, Nie et al. [38] used supercritical CO_2 to prepare a nanocomposite of HMX/AP in an RF matrix.

Spray drying was already discussed as a technique for generating nano-sized energetic materials, but the same technique has also been applied to produce e.g. RDX-based nanocomposite microparticles with PVAc or VMCC binders [17]. A solution of 5 wt%

RDX and 1 wt% binder in acetone at room temperature was spray-dried to produce the desired microparticles with nano-sized features. Similarly An et al. [18] obtained an LLM-105/estane 5703 nanocomposite by first dissolving the separate compounds in dimethylformamide and then spray drying the solution at elevated temperatures, leading to evaporation of the solvent. In this way spherical particles (granules) of 1-10 μm in diameter were formed consisting of a binder shell and LLM-105 nucleus. The average shell thickness was found to be about 20 nm. The core of each granule consisted of two or three practically spherical LLM-105 nanocrystals of about 50-100 nm in size.

Another class of nanocomposite energetic materials is prepared by using templates or substrates on which energetic materials are deposited or chemically bonded. Carbon nanotubes (CNTs) have been proposed by Ramaswamy et al. [39] to encapsulate energetic materials. CNTs are long, thin cylinders of carbon, first discovered by Iijima [51]. Typical dimensions of CNTs are a few nanometers in diameter and several microns in length. As a result of the very high electrical conductivity along the length of the CNT and their high thermal conductivity, CNTs have been identified as a candidate ingredient in energetic formulations [52]. In order to further improve the performance of CNTs as well as their dispersion in a polymer matrix, functionalized CNTs have been prepared by attaching functional groups like polyethyleneimine (PEI) and poly(methylmethacrylate) (PMMA) to the CNTs [53]. The hollow structure of CNTs or those of fullerene cages might be used to incorporate nano-energetic particles. For instance, Sharma et al. [54] looked into the computational possibilities for encapsulating polynitrogen clusters in C_{60} cage structures. Tse [40] showed the feasibility of encapsulating aluminum-containing

nanoparticles within CNTs during simultaneous growth using a robust flame synthesis process. Calculations predicted that energetic molecules like FOX-7 (1,1-diamino-2,2-dinitroethylene), RDX (hexahydro-1,3,5-trinitro-striazine), HMX (octahydro-1,3,5,7-tetranitro-1,3,5,7-tetrazocine), DHT (3,6-di(hydrazino)-1,2,4,5-tetrazine), DiAT (3,6-diazido-1,2,4,5-tetrazine), DAAT (3,3′-azo-bis(6-amino-1,2,4,5-tetrazine)), and five different N-oxides of DAAT can be stabilized inside a CNT, if a CNT of appropriate size is used [55]. FOX-7, RDX, and HMX were confined between graphene layers, again resulting in stabilization of these molecules.

3. Characterization

In the majority of the work presented in the previous section, the produced energetic nanomaterials have been characterized using a range of different analytical techniques. For the characterization of energetic nanomaterials in principle the same analytical techniques can be applied that are used for the characterization of conventionally sized materials. In this section some examples will be given of these characterization techniques, including a selection of literature references, as to illustrate the application of these techniques. The first part of this section will discuss the characterization of the nano-EMs themselves; the second part focuses on the characterization of formulations containing nano-EMs.

3.1 Characterization of energetic nanoparticles

3.1.1 Size, shape and surface area

Properties like mean size and shape of individual nanoparticles can be most easily visualized by means of scanning electron microscopy (SEM). In addition to SEM, scanning He-ion microscopy (SHIM) is gradually emerging as an alternative imaging technique which delivers images with subnanometer (0.75 nm) resolution combined with a tremendous depth-of-field, although its application as a characterization tool for energetic nanomaterials is still rather limited [56]. Using SEM in combination with image processing tools, allows assessment of the nanoparticle size distribution. An alternative is to use laser light scattering [9]. Transmission electron microscopy (TEM) has been applied in a limited number of cases; one should be aware that the high energy of the electron beam might easily lead to premature decomposition of the sample. Information on surface topography as well as size can be obtained using atomic force microscopy (AFM), as was applied e.g. by Frolov et al. [29] and Yang et al. [19].

The specific surface area of nanoparticles can be determined by a so-called BET-analysis, based on the adsorption of gas molecules (usually nitrogen) on a solid surface. This analytical method was used e.g. by Bishop et al. [27] to measure the specific surface area of PETN obtained by recrystallization from supercritical CO_2.

3.1.2 Crystal structure, identification and phase transitions

Crystallographic information and identification of the existence of different polymorphs or cocrystals can be obtained using X-ray diffraction (XRD) [7, 19]. Identification can be

achieved by means of spectroscopic techniques like FT-IR [22, 57] and Raman [7]. Using DSC and TG/DTA the endo- and exothermal properties like polymorphic phase transitions, melting and decomposition can be determined [57]. The same techniques can be applied to evaluate the compatibility between nanoparticles and other substances. In case of coated or encapsulated particles, surface analytical techniques like X-ray photon spectroscopy (XPS) are a valuable tool to investigate the composition of the coating layer [31]. SEM can be applied in combination with energy-dispersive X-ray spectroscopy (EDX) to qualitatively determine the elemental composition of a sample surface.

3.1.3 Internal defect structure and hazardous properties

The visualization of the internal defect structure which for conventionally sized energetic materials is traditionally done by means of optical microscopy [5] or confocal scanning laser microscopy [58] (CSLM) is practically impossible for energetic nanomaterials, since the submicron or nanometric particles are generally smaller than the resolution limit of these optical techniques (ca. 0.25 μm). Furthermore, the assessment of the sensitiveness of energetic nanomaterials, especially towards frictional stimuli, can yield erroneous results, as was outlined by Radacsi et al. [59].

Table 2: Impact and friction sensitivity of a selection of single-component and nanocomposite energetic materials.

Material	Impact sensitivity [a]	Friction sensitivity [b]	Reference
RDX			
400 μm	7.5 Nm	120 N	[10]
200-600 nm	10 Nm	> 360 N [c]	

Class 5 (< 450 μm) 4 μm 500 nm 200 nm	H_{50}: 23 cm H_{50}: 32 cm H_{50}: 73 cm H_{50}: 57 cm	- - - -	[28]
350 μm 200-900 nm	5 Nm 5 Nm	144 N > 360 N [c]	[12]
HMX			
50 nm [d] Conventional size (not specified) [d]	H_{50}: 24.4 and 26.4 cm H_{50}: 21.5 cm	- -	[6]
Conventional β-HMX (Class 6, 150 μm) γ-HMX ca. 1 μm (donut shape) γ-HMX 400 nm (spherical shape)	5 Nm 30 Nm 10 Nm	252 N > 360 N > 360 N	[10]
CL-20			
15 μm [e] 4 μm [e] 1 μm [e] 95 nm [e]	H_{50}: 25 cm H_{50}: 32 cm H_{50}: 40 cm H_{50}: 55 cm	6.4 kg 8 kg No reaction [c] No reaction [c]	[21]
30-100 μm [e] 300-700 nm [e]	H_{50}: 12.8 cm H_{50}: 37.9 cm	- -	[22]
Micron-sized (not specified) [f] 50-500 nm [f]	2.0 Nm < 1.56 Nm	79 N (crackling) Only discoloration reaction in the range of 28-192 N	[60]
α-NTO			
Micron-sized (not specified)	H_{50}: 26.2 cm	-	[19]
Needles: width 70-90 nm, length 200-300 nm	H_{50}: 35.5 cm	-	
RDX/TNT			
Micro-RDX/TNT 30/70 [g] Micro-RDX/TNT 50/50 [g] Micro-RDX/TNT 70/30 [g] Micro-RDX/TNO 100/0 [g] Nano-RDX/TNT 30/70 [h] Nano-RDX/TNT 50/50 [h]	12.26 Nm 9.81 Nm 5.89 Nm 2.45 Nm 7.35 Nm 4.9 Nm	96 N 96 N 72 N 160 N 144 N 120 N	[60]

Nano-RDX/TNT 70/30 [h]	2.94 Nm	144 N	
Nano-RDX/TNT 100/0 [h]	3.92 Nm	168 N	
RDX/GAP			
RDX (100%)	H_{50}: 12.8 cm	-	[49]
RDX [i]/GAP physical blend 40/60 wt%	H_{50}: 15.59 cm	-	
RDX (ca. 14 nm)/GAP nanocomposite 40/60 wt%	H_{50}: 30.2 cm	-	
PETN/SiO_2			
PETN (size not specified)/SiO_2, physical blend (ratio not specified)	H_{50}: 17 cm	-	[47]
PETN (size not specified)/SiO_2 90/10 wt%	H_{50}: 133 cm	-	
AP/RDX/SiO_2			
AP (size not specified)	H_{50}: 38.2 cm	-	[36]
RDX (size not specified)	H_{50}: 23.3 cm	-	
AP/RDX/SiO_2, with 4 wt% SiO_2 (ratio AP/RDX not specified; mean size of the AP and RDX particles ca. 60-100 nm)	H_{50}: 36.5 cm	-	
LLM-105			
LLM-105 (3-5 μm)	H_{50}: 70.5 cm	-	[18]
LLM-105 (50-100 nm)/estane nanocomposite	H_{50}: 112.6 cm	-	

[a] Impact sensitivity values can only be compared within the same data set; comparison of values between different data sets is not possible due to differences in test set-up and/or test method. Values are given in either Nm or in cm; the latter value corresponds to the H_{50} value, i.e. the drop height for which the initiation probability is 50%.

[b] Friction sensitivity values can only be compared within the same data set; comparison of values between different data sets is not possible due to differences in test set-up and/or test method. Values are given in N or in kg.

[c] Difficulties with measuring friction sensitivity of submicron particles, see Radacsi et al. [59] on the reliability of sensitivity test methods for submicron-sized RDX and HMX particles, more details in the text.

[d] The nano-HMX consisted of a mixture of β- and γ-HMX, whereas the conventionally sized HMX was pure β-HMX.

[e] ε-CL-20.

[f] β-CL-20.

[g] Physical mixture of ~5 μm RDX and ~5-10 μm TNT needles and ~3 μm TNT spheres.

[h] Spray-dried solution containing RDX and TNT in specified mass ratios; mean size RDX < 350 nm; mean size TNT needles 10-50 μm.

[i] Size not specified.

In Table 2 sensitivity data have been compiled of a range of nano- and micron-sized energetic materials. It is important to notice that impact and friction sensitivity values can only be compared within the same data set. Comparison of values between different data sets is not possible due to differences in test set-up and/or test method. Details on the used test methods can be found in the literature references mentioned in Table 2. Overall it can be stated that energetic nanomaterials are less sensitive towards impact and friction stimuli when compared to micron-sized particles, although some exceptions have been reported. For instance nano-β-CL-20 and nano-RDX/TNT samples from Risse et al. [60] were found to be more impact sensitive than their micron-sized counterparts. For the RDX/TNT samples this was attributed to the needle-like shape of the TNT crystals (10-50 μm needle length), which presence appeared to be more pronounced in the nano-samples. These needles might be more sensitive to impact than common TNT. Stepanov et al. [28] found indications of an optimum value for the impact sensitivity of RDX, where a 500 nm RDX product was found to be less impact sensitive than 200 nm RDX. Such an optimum was also reflected in the shock initiation tests of these samples (see Table 3).

With regard to the sensitivity testing of submicron or nano-sized energetic materials, there are some doubts about the reliability of particularly the friction sensitivity test [59]. The submicron or nano-sized crystals become distributed among the grooves of the porcelain plate that is used for the friction test (according to UN Test Series 3(b)(i) [61]), see Figure 5. This effect could explain the very high friction values found for e.g.

submicron or nano-sized RDX, HMX and CL-20, i.e. > 360 N, which is the maximum frictional force that can be exerted on the sample (see Table 2). Such extreme insensitiveness can thus be misleading, because apparently the measurement set-up is not suited for such small particles.

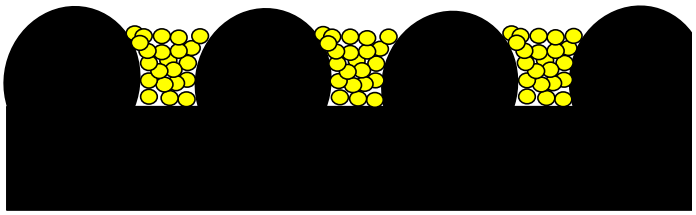

Figure 5: Schematic cross-section of a porcelain plate with 500 nm crystals distributed among the grooves [59].

3.1.4 Thermal analysis

Apart from the influence of particle size on sensitivity, size may affect the melting and/or decomposition temperatures. For instance Pivkina et al. [57] reported a lowering of the melting temperature of 50 nm RDX compared to micron-sized RDX using TG/DTA techniques: 190 °C vs. 200 °C, respectively. Similarly, also the decomposition temperature was found to be considerably lower in case of the nanometric RDX (220 °C) compared to conventionally sized RDX (235 °C). For nanometric AN (ca. 50 nm) all polymorphic phase transitions as well as the melting temperature were found to be shifted to lower temperatures when compared to the endothermal peaks found in 200 μm AN [57]. This lowering of the endo- and exothermal temperatures is attributed to the increase in the ratio of surface to bulk molecules, as a result of the very high specific surface area of nanoparticles. The number of neighboring molecules of a bulk molecule is larger than

that of a surface molecule, and this means that a surface molecule will be less bound to the structure than a bulk molecule. This leads to a lower onset of the melting/decomposition temperature.

3.2 Characterization of formulations containing energetic nanoparticles

The majority of the current literature focuses on the characterization of the chemical and physical properties of either the individual submicron-/nanoparticles or the nanocomposites (see previous section) and so far much less on the assessment of the properties on the level of a typical propellant or explosive composition in which energetic nanomaterials have been applied. A positive exception is the application of nanometric fuels (e.g. nano-aluminium) in propellant, explosive and pyrotechnic formulations; however, these type of nanomaterials have been excluded from the scope of this review. In case of the application of energetic nanomaterials as discussed in this review, the ballistic (e.g. energy release rate, burning rate, reaction rate, performance), sensitivity, mechanical and thermal stability/ageing characteristics appear to be the most important properties of interest. The assessment of these properties can be done by standard characterization techniques like strand burner, friction -/impact -/ESD-sensitivity/shock initiation, DMA/tensile and DSC/TG/DTA tests, respectively. Literature on the determination of these properties on the level of typical propellant or explosive compositions is rather limited, but there are a few exceptions which will be mentioned here.

3.2.1 Burning rate

In general the most prominent differences in characteristics between conventionally sized and nanometric particles are their ballistic, sensitivity and thermal properties. Similar to burning rates of pyrotechnic formulations containing nanomaterials, it can be expected that the burning rate of energetic nanomaterials is much higher than that of their conventional counterparts. Unfortunately, only limited data have been found in the literature that confirm this. When measuring the linear burning rate of pressed pellets of RDX powder (both with 10% porosity), Pivkina et al. [30] showed that at 10 MPa, the burning rate of 50 nm RDX was twice as high compared to that of 200 micron RDX: 30 versus 15.1 mm/s, respectively.

3.2.2 Shock initiation

Stepanov et al. [28] and Qiu et al. [17] investigated the shock initiation pressure of pressed explosive compositions in which conventionally sized RDX was replaced with nano-RDX, see Table 3. Both studies used the small-scale gap test (SSGT) requiring samples pressed into brass cylinders with the following dimensions: an internal diameter of 5.08 mm, an outer diameter of 25.4 mm and a height of 38.1 mm. In the work of Qiu et al. [17], shock initiation pressures of pressed samples consisting of spray-dried RDX/PVAc and RDX/VMCC (both 83/17 wt%) were found to be 4.0 and 3.3 GPa, respectively, whereas the reference sample RDX/VMCC (83/17 wt%) consisting of 4 μm RDX had a shock initiation pressure of only 2.5 GPa. Although the RDX in the VMCC-based compositions contained a substantially higher amount of HMX (9 wt%) compared to the RDX in the PVAc composition (4 wt%), which might contribute to the higher value of the shock initiation pressure, the unique nanostructure of the spray dried

microparticles, including the small RDX crystal size and uniform mixing of RDX crystals with binder were regarded to be the main factors enabling this extremely low shock initiation pressure [17].

Table 3: Shock initiation data for RDX-containing pressed samples.

Composition	Mean size RDX	TMD [%]	Density [g/cm^3]	Shock initiation pressure [GPa]	Reference
RDX [a]/VMCC (slurry coated), 83/17 wt%	4 µm	93.7	1.64	2.5	[17]
RDX [b]/PVAc (spray dried), 83/17 wt%	100-200 nm	91.9	1.58	4.0	
RDX [a]/VMCC (spray dried), 83/17 wt%	100-200 nm	92.5	1.62	3.3	
RDX [c]	Class 1 (ca. 150 µm)	89.0	1.6	1.1	[28]
RDX [c]	4 µm	81.5	1.49	2.0	
RDX [d]	500 nm	78.6	1.43	2.6	
RDX [d]	200 nm	78.0	1.42	2.1	
RDX [c]/wax, 88/12 wt%	Class 1 (ca. 150 µm)	94.9	1.69	2.0	
RDX [c]/wax, 88/12 wt%	4 µm	87.4	1.57	2.1	
RDX [d]/wax, 88/12 wt%	500 nm	88.6	1.58	3.2	
RDX [d]/wax, 88/12 wt%	200 nm	88.0	1.57	2.5	
RDX [e,d]/wax, 88/12 wt%	4 µm + 200 nm (ratio not specified)	91.0	1.62	2.2	

[a] HMX content of 9 wt%.

[b] HMX content of 4 wt%.

[c] Commercial RDX: HMX content of ~10 wt%.

[d] Recrystallized RDX: HMX content of ~2 wt%.

Similar results by Stepanov et al. [28] showed that the shock initiation pressure of pressed RDX/wax (88/12 wt%) samples were also higher for samples containing the nano-sized RDX compared to samples containing conventionally sized RDX or a mixture of nano- and micron-sized RDX. An interesting and unexpected result in the study of Stepanov et al. [28], was the reversal of the sensitivity trend with the RDX crystal size when going from 500 nm to 200 nm. This finding suggests that re-sensitization occurs below a certain crystal size. It may also be indicative of a transition to a different initiation mechanism below a certain crystal size.

The results of the characterization of energetic nanomaterials and nanocomposites show that the foreseen applications of energetic nanomaterials focus primarily on polymer bonded explosives (PBX), solid composite rocket propellants and gun propellants aiming for reduced sensitivity (specifically for explosives), higher solid loads and hence higher performances, and higher energy release rates.

Nanomaterials are also applied in pyrotechnic formulations, however, these are mainly limited to nanopowders of metals and metal oxides (so-called nanothermites). These nanomaterials were excluded from the scope of this review. More information on these classes of compositions is available in literature [4].

4. Development challenges

One question that follows from this literature review is why there is hardly any scale-up of the most promising single-component and/or nanocomposite energetic materials? Academic research is still mainly focused on trying to explore the numerous possibilities

in this domain, trying to understand the influence of the processing conditions on the product properties and to be able to optimize and control the production process.

The current developments of CHNO-based energetic nanomaterials appear to be limited to small scale production techniques to either make nanoparticles directly or by making nanoparticles which are embedded in a polymer matrix (so-called sol-gel). Although benefits in the area of less sensitivity (increased safety) and higher solid loads (increased performance) have been demonstrated, economically viable, scaled up production processes have only rarely been addressed so far. This is probably one of the reasons that intermediate scale application of energetic nanomaterials in typical propellant and explosive formulations is currently very limited. A further reason prohibiting progress could be that a commonly shared view on the economic benefits of energetic nanomaterials and production processes is lacking.

A considerable number of technical challenges can be expected when trying to apply energetic nanomaterials in a formulation. For instance, when replacing conventionally sized energetic materials with their submicron/nanometric counterparts in a polymer matrix, the wetting of the particles by the polymer is expected to be rather limited which may negatively affect the solid load. Coagulation effects of nanomaterials might be detrimental to the high reaction rates and reduced sensitivities typically found for nanomaterials. The conventional processing techniques for the mixing and casting of polymer bonded compositions using a planetary mixer might not be suitable anymore when processing energetic nanomaterials in a formulation. Resonant acoustic mixing

might be an emerging alternative technique, being a much more intensive method for the processing of solid/solid and solid/liquid mixtures, where microscale mixing occurs and mixing times can be reduced significantly [62]. Resonant acoustic mixing (RAM) might therefore gradually replace conventional mixing/casting techniques in the future.

The use of nanomaterials may involve health and environmental issues as a result of physical properties like particle size, shape and specific surface area, even though the chemical nature of the compound itself may be non-toxic. This is related to potential adverse effects of nanoparticles on the lungs, including oxidase stress, inflammation, fibrosis and genotoxicity [63], especially for materials which are insoluble in water. Another potential disadvantage of energetic nanomaterials is the lower thermal stability due to the observed shift to lower melting and decomposition temperatures compared to micron-sized materials [64]. This may lead to an enhanced susceptibility to ageing due to thermal loads or thermal cycling. If the activation energy and/or the frequency factor of the decomposition reaction (assuming an Arrhenius dependence) of an energetic nanomaterial changes, this may affect the shelf life of compositions containing energetic nanomaterials.

It could be helpful to first try to answer the following question: what is the benefit of applying nanoenergetics? In order to answer this question the following aspects should considered: the benefits, risks and costs involved with the (partial) replacement of conventionally sized energetic materials by energetic nanomaterials (down-selection of application domains), the required production volumes – depending on the application

area – and the benefits/risks/costs involved in selecting and scaling up the production technique that would be best suited for manufacturing a specific energetic nanomaterial. The envisioning of new application areas of nanoenergetics outside the defense domain, e.g. medicine, optics, electronics, etc. could open up possibilities for sharing development costs as well as new product development and innovation by multidisciplinary "cross-overs". This approach could therefore provide a means to select areas for which it would be economically beneficial to invest in. However, such a business case can only be prepared if it is supported by relevant (experimental) data. Since the mostly academic literature in this area is still mainly focused on the exploration of small scale production techniques to prepare energetic nanomaterials, a thorough evaluation of the benefits, risks and costs involved with the (partial) replacement of conventionally sized energetic materials by nanomaterials is lacking. This is considered as the main obstacle that stagnates the industrial implementation and large scale application of energetic nanomaterials.

Based on the current status of the research and development on energetic nanomaterials as outlined in this review, the following technical challenges and a potential strategy to manage these challenges can be identified:

- **Scale-up**: currently developed small scale techniques for producing energetic nanomaterials like (electro)spray using nozzles are difficult to scale up; of course more nozzles can be used, but this is scaling out rather than scaling up; an exception might be the spray flash evaporation process developed by Risse et al. [11], which can be operated continuously. In addition to spray flash evaporation also bead milling and resonant

acoustic mixing have been identified as a promising means for large-scale production of nano-sized energetic cocrystals.

- **Thermal stability**: as particle size decreases, also the melting point and decomposition temperature have been found to decrease; this is an intrinsic property which might negatively affect the susceptibility to ageing of compositions in which energetic nanomaterials have been applied.

- **Processing of nanoparticles**: the processing of energetic nanomaterials in polymeric binders might lead to highly viscous compositions due to problems with the wetting of the nanoparticles. This might require a different, more intensive mixing technique than the currently used planetary mixers; resonant acoustic mixing could be a promising alternative. Production of composites like those produced with sol-gel techniques rather than individual energetic nanomaterials, might be a feasible way-forward to circumvent these processing problems. Furthermore, functionalization of nanoparticles by applying a coating to improve their dispersion and wettability in a polymeric binder, to prevent coagulation or to modify their reactivity or ignitability could also enhance a more widespread application of energetic nanomaterials. A technique such as atomic layer deposition (ALD) combined with a fluidized bed reactor – which is well-suited for large scale operations – as a means to coat (nano)particles, has matured significantly over the past decade [65, 66].

- **Characterization techniques**: the majority of the characterization techniques that are applied to conventional energetic materials, can also be used in case of energetic

nanomaterials, except techniques to assess the internal defect content. At present, this latter characteristic of an energetic nanomaterial can only be assessed indirectly, e.g. by determining its sensitivity towards impact, friction and shock.

- **Storage and transport**: for transport purposes, explosives are generally wetted with at least 15 wt% water to reduce friction and impact sensitivity. Drying of these wetted particles might lead to coagulation effects of the nanoparticles, which could be detrimental to the specific properties that result from their nanometric size. The production of composites like those produced with sol-gel techniques rather than individual energetic nanomaterials, might solve these storage, transport and coagulation problems.

- **Toxicity**: even though the chemical nature of the compound itself may be non-toxic, the use of nanomaterials may involve health and environmental issues as a result of physical properties like particle size, shape and specific surface area.

The proposed technical solutions to manage the challenges identified above, may contribute to a better understanding of the benefits, risks and costs involved in the use and scale-up of energetic nanomaterials and, if considered economically feasible, a more widespread application of these nanomaterials in the defense and space domains.

Acknowledgements

The author acknowledge financial support from the Netherlands Ministry of Defense and the European Defense Agency (EDA) program Energetic Materials Towards an Enhanced European Capability (EMTEEC), Contract No B-1453-GEM2-GC-NL-1.

References

1 I. Uddin, S. Venkatachalam, A. Mukhopadhyay and M.A. Usmani, Nanomaterials in the pharmaceuticals: occurrence, behaviour and applications (review), Curr. Pharm. Des. **22** (2016) 1472-84.

2 S. Raj, S. Jose, U.S. Sumod and M. Sabitha, Nanotechnology in cosmetics: opportunities and challenges (review), J. Pharm. Bioallied Sci. **4** (2012) 186-193.

3 N. Sharma, H. Ojha, A. Bharadwaj, D.P. Pathak and R.K. Sharma, Preparation and catalytic applications of nanomaterials: a review, RSC Adv. **5** (2015) 53381-53403.

4 V.E. Zarko and A. Gromov (eds.), in: Energetic Nanomaterials - Synthesis, Characterization, and Application, ISBN: 978-0-12-802710-3, Elsevier Inc. 2016.

5 A.E.D.M. van der Heijden and R.H.B. Bouma, Crystallization and characterization of RDX, HMX and CL-20, Crystal Growth & Design **4** (2004) 999-1007.

6 Z. Yongxu, L. Dabin and L. Chunxu, Preparation and characterization of reticular nano-HMX, Propellants, Explosives, Pyrotechnics **30** (2005) 438-441.

7 M.A. Barreto-Cabán, L. Pacheco-Londoño, M.L. Ramírez and S.P. Hernández-Rivera, Novel method for the preparation of explosives nanoparticles, Sensors,

and Command, Control, Communications, and Intelligence (C3I) Technologies for Homeland Security and Homeland Defense V, E.M. Carapezza (ed.), Proc. of SPIE **6201** (2006) 620129.

8 A.E.D.M. van der Heijden, C.P.M. Roelands, Y.L.M. Creyghton, E. Marino, R.H.B. Bouma, J.H.G. Scholtes and W. Duvalois, Energetic (nano)materials: crystallization, characterization and insensitive plastic bonded explosives, Propellants, Explosives, Pyrotechnics **33** (2008) 25-32.

9 D. Spitzer, M. Comet, C. Baras,V. Pichot and N. Piazzon, Energetic nano-materials: opportunities for enhanced performances, J of Phys and Chem of Solids **71** (2010) 100-108.

10 N. Radacsi, A.I. Stankiewicz, Y.L.M. Creyghton, A.E.D.M. van der Heijden and J.H. ter Horst, Electrospray crystallization for high quality submicron-sized crystals, Chemical Engineering & Technology **34** (2011) 624-630.

11 B. Risse, D. Spitzer, D. Hassler, F. Schnell, M. Cometa, V. Pichot and H. Muhr, Continuous formation of submicron energetic particles by the flash-evaporation technique, Chemical Engineering Journal 203 (2012) 158-165.

12 N. Radacsi, A.E.D.M. van der Heijden, A.I. Stankiewicz and J.H. ter Horst, Cold plasma synthesis of high quality organic nanoparticles at atmospheric pressure, Journal of Nanoparticle Research **15** (2013) 1445.

13 D.D. Dlott, Thinking big (and small) about energetic materials, Materials Science and Technology **22** (2006) 463.

14 K. Zhang, P. Alphonse and C. Tenailleau, Nano energetic materials: synthesis, characterization, modeling and application, in: Energetic Materials: Chemistry, Hazards, and Environmental Aspects, J.R. Howell and T.E. Fletcher (eds.), ISBN: 978-1-60876-267-5, Nova Science Publishers, Inc. (2010).

15 X. Zhou, M. Torabi, J. Lu, R. Shen and K. Zhang, Nanostructured energetic composites: synthesis, ignition/combustion modeling, and applications, Appl. Mater. Interfaces **6** (2014) 3058-3074.

16 F. Pessina and D. Spitzer, The longstanding challenge of the nanocrystallization of 1,3,5-trinitroperhydro-1,3,5-triazine (RDX), Beilstein J. of Nanotechnology **8** (2017) 452-466.

17 H. Qiu, V. Stepanov, A.R. Di Stasio, T. Chou and W.Y. Lee, RDX-based nanocomposite microparticles for significantly reduced shock sensitivity, J Hazard Mat **185** (2011) 489-493.

18 C. An, H. Li, X. Geng, J. Li and J. Wang, Preparation and properties of 2,6-diamino-3,5-dinitropyrazine-1-oxide based nanocomposites, Propellants Explosives Pyrotechnics **38** (2013) 172-175.

19 G. Yang, F. Nie, J. Li, Q. Guo and Z. Qiao, Preparation and characterization of nano-NTO explosive, Journal of Energetic Materials **25** (2007) 35-47.

20 Y. Bayat, M. Eghdamtalab and V. Zeynali, Control of the particle size of submicron HMX explosive by spraying in non-solvent, Journal of Energetic Materials **28** (2010) 273-284.

21 Y. Bayat and V. Zeynali, Preparation and characterization of nano-CL-20 explosive, Journal of Energetic Materials 29 (2011) 281-291.

22 J. Wang, J. Li, C. An, C. Hou, W. Xu and X. Li, Study on ultrasound- and spray-assisted precipitation of CL-20, Propellants Explosives Pyrotechnics **35** (2010) 1-6.

23 D. Doblas, M. Rosenthal, M. Burghammer, D. Chernyshov, D. Spitzer and D.A. Ivanov, Smart energetic nano-sized cocrystals: exploring fast structure formation and decomposition, Cryst. Growth Des. **16** (2016) 432-439.

24 H. Qiu, R.B. Patel, R.S. Damavarapu and V. Stepanov, Nanoscale 2CL-20.HMX high explosive cocrystal synthesized by bead milling, CrystEngComm **17** (2015) 4080-4083.

25 G. Zeng, W. Pang and J. Zhou, Preparation and characterization of TATB based nanocomposites, Procedia Engineering **102** (2015) 610-614.

26 M.A. Reus, G. Hoetmer, A.E.D.M. van der Heijden and J.H. ter Horst, Concomitant crystallization for in situ encapsulation of organic materials, Chemical Engineering and Processing **80** (2014) 11-20.

27 R.L. Bishop, J.F. Kramer and R.L. Flesner, Production of very-high surface area PETN by recrystallization from supercritical CO_2, LA-UR-99-5000, presented at Life Cycles of Energetic Materials, Orlando, Florida, USA, Sept. 1999.

28 V. Stepanov, V. Anglade, W.A. Balas Hummers, A.V. Bezmelnitsyn and L.N. Krasnoperov, Production and sensitivity evaluation of nanocrystalline RDX-based explosive compositions, Propellants Explosives Pyrotechnics 36 (2011) 240-246.

29 Yu. Frolov, A. Pivkina, P. Ulyanova and S. Zavyalov, Nanomaterials and nanostructures as components for high-energy condensed systems, Proceedings of the 37th International Pyrotechnics Seminar (EUROPYRO 2011) and 10th International GTPS Seminar, 17-19 May 2011, Reims, France.

30 A. Pivkina, P. Ulyanova, Yu. Frolov, S. Zavyalov and J. Schoonman, Nanomaterials for heterogeneous combustion, Propellants Explosives Pyrotechnics **29** (2004) 39.

31 G. Yang, H. Hu, Y. Zhou, Y. Hu, H. Huang, F. Nie and W. Shi, Synthesis of one-molecule-thick single-crystalline nanosheets of energetic material for high-sensitive force sensor, Sci. Rep. **2** (2012) 698.

32 J. Wang, Y. Wang, Z. Qiao, L. Zhang, P. Wu and G. Yang, Self-assembly of TATB 3D architectures via micro-channel crystallization and a formation mechanism, CrystEngComm **18** (2016) 1953.

33 B.C. Tappan and T.B. Brill, Thermal decomposition of energetic materials 86. Cryogel synthesis of nanocrystalline CL-20 coated with cured nitrocellulose, Propellants Explosives Pyrotechnics **28** (2003) 223.

34 T.B. Brill, B.C. Tappan and J. Li, Synthesis and characterization of nanocrystalline oxidizer/monopropellant formulations, MRS Proceedings **800** (2004) AA2.1.

35 P. Holub and P. Vávra, Preparation of nanostructured energetic materials by sol-gel technology, Scientific Papers of the University of Pardubice, Series A, Faculty of Chemical Technology **11** (2005) 177.

36 R. Chen, Y. Luo, J. Sun and G. Li, Preparation and properties of an AP/RDX/SiO_2 nanocomposite energetic material by the sol-gel method, Propellants Explosives Pyrotechnics **37** (2012) 422-426.

37 A. Wuillaume, A. Beaucamp, F. David-Quillot and C. Eradès, Formulation and characterizations of nanoenergetic compositions with improved safety, Propellants Explosives Pyrotechnics **39** (2014) 390-396.

38 F. Nie, J. Zhang, Q. Guo, Z. Qiao and G. Zeng, Sol-gel synthesis of nanocomposite crystalline HMX/AP coated by resorcinol-formaldehyde, J. of Phys. and Chem. of Solids **71** (2010) 109-113.

39 A.L. Ramaswamy, P. Kaste, A.W. Miziolek, B. Homan, S. Trevino and M.A. O'Keefe, Nanoenergetics weaponization and characterization technologies, ACS Symposium Series **891** (2005) 180-196.

40 S.D. Tse, STIR: Encapsulating reactive nanoparticles in carbon nanotubes using flame-based synthesis, Final report 2008.

41 L. Rayleigh, On the equilibrium of liquid conducting masses charged with electricity, Phil. Mag. **14** (1882) 184.

42 S. Aitipamula, R. Banerjee, A.K. Bansal, K. Biradha, M.L. Cheney, A.R. Choudhury, G. R. Desiraju, A.G. Dikundwar, R. Dubey, N. Duggirala, P.P. Ghogale, S. Ghosh, P.K. Goswami, N.R. Goud, R.R.K.R. Jetti, P. Karpinski, P. Kaushik, D. Kumar, V. Kumar, B. Moulton, A. Mukherjee, G. Mukherjee, A. S. Myerson, V. Puri, A. Ramanan, T. Rajamannar, C.M. Reddy, N. Rodriguez-Hornedo, R.D. Rogers, T.N. Guru Row, P. Sanphui, N. Shan, G. Shete, A. Singh,

C.C. Sun, J.A. Swift, R. Thaimattam, T.S. Thakur, R.K. Thaper, S.P. Thomas, S. Tothadi, V.R. Vangala, N. Variankaval, P. Vishweshwar, D.R. Weyna, M.J. Zaworotko, Polymorphs, Salts, and Cocrystals: What's in a Name?, Crystal Growth & Design **12** (2012) 2147-2152.

43 K.B. Landenberger and A.J. Matzger, Cocrystals of 1,3,5,7-tetranitro-1,3,5,7-tetrazacyclooctane (HMX), Cryst. Growth Des. **12** (2012) 3603-3609.

44 O. Bolton, L.R. Simke, P.F. Pagoria and A.J. Matzger, High power explosive with good sensitivity: a 2:1 cocrystal of CL-20:HMX, Cryst. Growth Des. **12** (2012) 4311-4314.

45 S.R. Anderson, D.J. am Ende, J.S. Salan and P. Samuels, Preparation of an energetic-energetic cocrystal using resonant acoustic mixing, Propellants Explosives Pyrotechnics **39** (2014) 637-640.

46 S.R. Anderson, P. Dubé, M. Krawiec, J.S. Salan, D.J. am Ende and P. Samuels, Promising CL-20-based energetic material by cocrystallization, Propellants Explosives Pyrotechnics **41** (2016) 783-788.

47 R.L. Simpson, T.M. Tillotson, L.W. Hrubesch and A.E. Gash, Nanostructured energetic materials derived from sol-gel chemistry, Proceedings of the Annual Conference of ICT, Karlsruhe, Germany, June 2000.

48 G. Li, L. Shen, B. Zheng, M. Xia and Y. Luo, The preparation and properties of AP-based nano-limit growth energetic materials, Advanced Materials Research **924** (2014) 105-109, ISSN: 1662-8985, Trans Tech Publications, Switzerland.

49 G. Li, M. Liu, R. Zhang, L. Shen, Y. Liu and Y. Luo, Synthesis and properties of RDX/GAP nano-composite energetic materials, Colloid Polym. Sci. **293** (2015) 2269-2279.

50 M. Jin, G. Wang, J. Deng, G. Li, M. Huang and Y. Luo, Preparation and properties of NC/RDX/AP nano-composite energetic materials by the sol-gel method, J. Sol-Gel Sci. Technol. **76** (2015) 58-65.

51 S. Iijima, Helical microtubules of graphite carbon, Nature **354** (1991) 56-58.

52 Q. Yan, M. Gozin, F. Zhao, A. Cohena and S. Pang, Highly energetic compositions based on functionalized carbon nanomaterials (review), Nanoscale **8** (2016) 4799.

53 M.S. Bratcher, B. Gersten, W. Kosik, H. Ji and J. Mays, A study in the dispersion of carbon nanotubes, Proc. of the Materials Research Society, Fall 2001.

54 H. Sharma, I. Garg, K. Dharamvir and V.K. Jindal, Nitrogen clusters inside C60 cage and new nanoscale energetic materials, (2009) https://arxiv.org/abs/0908.3412v1 (accessed April 19, 2018).

55 M. Smeu, F. Zahid, W. Ji, H. Guo, M. Jaidann and H. Abou-Rachid, Energetic Molecules Encapsulated Inside Carbon Nanotubes and between Graphene Layers: DFT Calculations, J Phys Chem C 115 (2011) 10985-10989.

56 A.E.D.M. van der Heijden, Y.L.M. Creyghton, R.J.E. van de Peppel and E. Abadjieva, Modification and characterization of (energetic) nanomaterials, Journal of Physics and Chemistry of Solids **71** (2010) 59-63.

57 A. Pivkina, Yu. Frolov, S. Zavyalov, P. Ul'yanova and J. Schoonman, Thermal properties of nano-sized energetic materials, in: Proceedings of 30th International Polytechnics Seminar, San Malo, France (2003) 555-571.

58 A.E.D.M. van der Heijden and R.H.B. Bouma, Confocal scanning laser microscopic study of the RDX defect structure in deformed polymer bonded explosives, Propellants Explosives Pyrotechnics **41** (2016) 875-882.

59 N. Radacsi, R.H.B. Bouma, E.L.M. Krabbendam-la Haye, J.H. ter Horst, A.I. Stankiewicz and A.E.D.M. van der Heijden, On the reliability of sensitivity test methods for submicrometer-sized RDX and HMX particles, Propellants Explosives Pyrotechnics **38** (2013) 761-769.

60 B. Risse, D. Spitzer, D. Hassler, F. Schnell and M. Comet, Continuous formation of nano energetic materials, Proceedings of the 37th International Pyrotechnics Seminar (EUROPYRO 2011) and 10th International GTPS Seminar, 17-19 May 2011, Reims, France.

61 UN Recommendations on the Transport of Dangerous Goods, ST-SG-AC10-11, UN Test Series 3(b)(i) BAM friction sensitivity.

62 J.G. Osorio and F.J. Muzzio, Evaluation of resonant acoustic mixing performance, Powder Technology **278** (2015) 46-56.

63 X. Lu, T. Zhu, C. Chen and Y. Liu, Right or left: the role of nanoparticles in pulmonary diseases, Int. J. Mol. Sci. **15** (2014) 17577-17600.

64 N. Zohari, M.H. Keshavarz and S.A. Seyedsadjadi, The advantages and shortcomings of using nano-sized energetic materials, Central European Journal of Energetic Materials **10** (2013) 135-147.

65 D.M. King, X. Liang and A.W. Weimer, Functionalization of fine particles using atomic and molecular layer deposition (review), Powder Technology **221** (2012) 13-25.

66 S. Salameh, J. Gómez-Hernández, A. Goulas, H. van Bui and J.R. van Ommen, Advances in scalable gas-phase manufacturing and processing of nanostructured solids: a review, Particuology 30 (2017) 15-39.